Vol. 552: 159–176, 2016
doi: 10.3354/meps11753

MARINE ECOLOGY PROGRESS SERIES
Mar Ecol Prog Ser

Published June 23

Wandering mussels: using natural tags to identify connectivity patterns among Marine Protected Areas

Inês Gomes[1,2,*], Laura G. Peteiro[1,3], Rui Albuquerque[1], Rita Nolasco[4], Jesús Dubert[4], Stephen Edward Swearer[5], Henrique Queiroga[1]

[1]Departmento de Biologia & CESAM, Universidade de Aveiro, Campus Universitario de Santiago, 3810-193 Aveiro, Portugal
[2]Marine Biology Research Group, Ghent University, 9000 Ghent, Belgium
[3]Departamento de Ecoloxía e Bioloxía Animal, Facultade de Ciencias do Mar, Universidade de Vigo, 36310 Vigo, Spain
[4]Departmento de Física and Centro de Estudos do Ambiente e do Mar (CESAM), Universidade de Aveiro, Campus Universitario de Santiago, 3810-193 Aveiro, Portugal
[5]School of BioSciences, University of Melbourne, Parkville, Victoria 3010, Australia

ABSTRACT: Knowledge of connectivity pathways in the marine environment is crucial for understanding the spatial structure of populations and for developing appropriate monitoring and management strategies. Here, we used the mussel *Mytilus galloprovincialis* as a model species to investigate connectivity patterns within the Berlengas and Arrábida Marine Protected Areas (MPAs) along the central Portuguese west coast. We generated an atlas of location-specific environmental markers based on the microchemistry of bivalve larval shells (using laser ablation inductively coupled plasma mass spectrometry). This atlas was then employed to trace the natal origins of newly settled mussels and generate connectivity matrices among populations. Our results reflected 3 distinctive chemical signatures in larval shells, corresponding to 3 regions: Estremadura, Cascais and Arrábida. Linear discriminant analyses allowed for a high reclassification success (average of 79.5% of jackknifed cross-validated cases correctly assigned) based on 8 of the 16 trace elements analyzed (B, P, Co, Cu, Zn, Ce, Pb and U). The population connectivity matrix identified different dispersal pathways for mussel larvae, in particular a predominantly northward dispersion pattern in July 2013. This pattern was consistent with simultaneous environmental physical data, which confirmed an extended period of wind reversal and upwelling relaxation. The Arrábida MPA was an important source population for the other 2 regions and showed high rates of self-recruitment but limited connectivity to the Berlengas MPA. These direct measures of demographic connectivity can be a powerful tool to inform policymakers on the conservation and management of ecologically coherent networks of protected areas in coastal marine ecosystems.

KEY WORDS: Natal site atlas · *Mytilus* · Elemental composition · LA-ICP-MS · Connectivity

INTRODUCTION

Measuring the spatial extent over which marine subpopulations are connected by larval dispersal is a fundamental issue in marine metapopulation studies (Pineda et al. 2007) and in defining the relevant spatial scales for area-based conservation measures (Gaines et al. 2010). Evidence from various fields such as physical oceanography, biophysical modelling, molecular genetics and the geochemistry of site-specific natural tags has been used to quantify connectivity at different spatial and temporal scales. Indeed, natural tags, such as the geochemical composition of calcified structures of marine organisms, are increasingly being employed as a strategic tool in marine research. These naturally induced marks

*Corresponding author: istgomes@gmail.com

have frequently been used in paleo-environmental research in coral skeletons (Mitsuguchi et al. 1996), foraminiferal shells (Keul et al. 2013) and ostracod shells (Börner et al. 2013). More recently, they have been applied to determine natal signatures and dispersal patterns, using crustacean embryos and larvae (DiBacco & Levin 2000, Carson 2010), fish otoliths (e.g. Swearer et al. 1999), larval mollusk statoliths (Zacherl 2005) and shells (e.g. (Becker et al. 2007, Carson 2010). This method requires not only the existence of location-specific chemical signatures at the site of origin but also the maintenance of these 'natal tags' after settlement (Thorrold et al. 2007). Both physical and biological properties of the marine environment can influence the incorporation of such chemical signatures in biogenic carbonates at spatial scales over which they allow discrimination among natal sites (Campana 1999). Yet, the lack of a clear relationship between seawater chemistry and elemental composition of calcified structures (Campana & Thorrold 2001, Warner et al. 2005) might also reflect genetic (Chittaro et al. 2006) and/or maternal (Lloyd et al. 2008) effects on elemental signatures.

Assembling regional chemical reference maps of natal origins based on geographical differences in biogenic carbonate chemistry can be used as a tracking method (Becker et al. 2007). However, to successfully set up a suitable natal site atlas, it is crucial to consider not only the larval life history and potential dispersal scales, but also the local geology, anthropogenic pressures and oceanography of the study region (Miller et al. 2013). This approach has already led to important progress in our understanding of metapopulation connectivity in coral reef ecosystems (Swearer et al. 1999, Chittaro & Hogan 2013), estuarine areas (Swearer et al. 2003, Carson et al. 2010) and open coast environments (Warner et al. 2005, Becker et al. 2007, Cook et al. 2014). Although the dispersal of planktonic larvae of benthic invertebrates has been studied systematically, the specific link between small-scale coastal geography and larval supply is less well resolved (Adams et al. 2014). In the eastern boundary of upwelling systems, sinuous coastlines and topographic features, such as the presence of capes and associated bays, can influence the degree of population connectivity, through interactions between regional upwelling/downwelling processes and local-scale topography (Siegel et al. 2008). Elemental fingerprinting is increasingly being applied to understand connectivity patterns in complex environments because of its potential to detect not only bay–open coast dispersal patterns (Becker et al. 2007, Sorte et al. 2013, Carson 2010) but also along-shore interchanges between populations in upwelling systems (López-Duarte et al. 2012). Coastal upwelling systems around the world have been extensively studied because of their high productivity and the physical mechanisms involved in along- and cross-shore larval transport (Roughgarden et al. 1988, Wing et al. 1995, Shanks & Brink 2005, Narváez et al. 2006, Morgan et al. 2009). In the western Iberia upwelling ecosystem, several studies have highlighted the importance of variability in the frequency and intensity of upwelling episodes to larval dispersal and recruitment of a diversity of invertebrate species (Queiroga et al. 2007, Peteiro et al. 2011, Nolasco et al. 2013a). However, large-scale studies on invertebrate larval dispersal pathways remain in the dominion of simulation modelling (Domingues et al. 2012, Nolasco et al. 2013a), and might not reflect local-scale connectivity patterns. Small-scale topographic features can influence the degree of population connectivity by generating different hydrodynamic stress amongst open coasts and protected embayments (Nicastro et al. 2008, Carson 2010).

Present theoretical frameworks and binding agendas at international (Convention on Biological Diversity) and European (OSPAR Commission, Marine Strategy Framework Directive) levels are advocating for the establishment of ecologically coherent MPA networks by 2020. Population connectivity is one of the 4 assessment criteria proposed to evaluate the degree of ecological coherence of systems of protected areas (Ardron 2008), with important implications for the persistence and resilience of metapopulations (White et al. 2010). In Portugal, however, an estimate of population connectivity among MPAs is yet to be accomplished. Therefore, regional-specific scientific input on ecological patterns of connectivity, operating at a suitable temporal and spatial scale, is crucial if we are to deliver effective outcomes to established conservation policy targets.

Here we focus on the central west coast of Portugal, which encompasses 2 MPAs included in the European ecological network of protected areas Natura 2000. Although both MPAs in this study were initially established in a broad biodiversity conservation and fishery management context, single-species quantitative measurements of connectivity are important to identify the best range of reserve spacing that can maximize benefits for marine larvae with potential large-scale dispersal among habitat patches. *Mytilus galloprovincialis* has been largely employed as a model species to study connectivity patterns between subpopulations because of its broad distribution and its function as an ecosystem engineer

(Becker et al. 2007, Fodrie et al. 2011, López-Duarte et al. 2012). Our objective was to determine the spatial resolution of geochemical signatures in *M. galloprovincialis* larval shells to reveal connectivity patterns between MPAs and adjacent areas. The complex topography of the coastline, characterized by prominent capes, bays and estuaries, represents an interesting setting for microchemistry-based investigations. Natural tags were investigated in a snapshot manner in summer 2013, using a large-scale and short-term static atlas of elemental variability in mytilid larval shells. This reference map was employed to reconstruct the natal origin of newly settled mussels, under complex circulation patterns during the typical spring–summer upwelling season when northerly winds off Western Iberia usually prevail and cause upwelling of cold and nutrient-rich waters (Relvas et al. 2007). We further integrate and compare the results with simultaneous environmental physical data, to assess whether the patterns we observed (geochemical fingerprints and dispersal pathways) were consistent with trace elemental composition, oceanography and hydrographic conditions of the area. Our results confirm the feasibility of the technique to accurately quantify self-recruitment and connectivity among MPAs, at ecologically relevant scales, within the complex coastal topography and bathymetry of the central Portuguese west coast.

MATERIALS AND METHODS

Species description

In Europe, the Mediterranean mussel (*Mytilus galloprovincialis* Lamarck, 1819) is distributed throughout the Mediterranean and along the Atlantic coast as far north as northwestern Ireland (Gardner 1992). It was chosen as a model species as it is widely distributed in temperate marine rocky shores, making it particularly suitable to assess environmentally related signatures. Also, as an important structural component of rocky intertidal ecosystems, mussels play a key role as ecosystem engineers, increasing microhabitat complexity, environmental heterogeneity and benthic species richness with significant influence at the ecosystem level (Borthagaray & Carranza 2007). Along the central coast of Portugal, mussels are subjected to an informal traditional fishery, depending largely on site accessibility, to supplement diet or for commerce or bait (Rius & Cabral 2004).

As *M. galloprovincialis* are broadcast-spawning invertebrates, fertilization occurs in the water column, leading to a series of free-swimming planktotrophic larval stages (Bayne 1976). Shell mineralization starts approximately 20 h after fertilization, forming prodissoconch I, which enlarges until the trochophore is completely enfolded, forming the D-veliger (24–48 h after fertilization; Ruiz et al. 2008). Primary settlement sets the beginning of the juvenile form, and occurs when pediveliger larvae metamorphose and selectively anchor onto benthic surfaces by secreting byssal threads. The final step of settlement in bivalves is manifested after metamorphosis by a change in shell morphology and composition, with a differentiation of the prodissoconch (larval shell) and the dissoconch (benthic shell). Although planktonic larval development and duration (PLD) are strongly dependent on temperature and food availability, *M. galloprovincialis* larvae stay in the plankton for ~2–4 wk (Ruiz et al. 2008), with the possibility to delay metamorphosis if suitable settlement substrates are not available (Chicharo & Chicharo 2000). Philippart et al. (2012) investigated the presence of mytilid larvae in European coastal waters as a proxy for time of reproduction and reported a seasonal pattern for the Iberian coast with 1 major peak in spring and a less significant peak during the fall.

Area description

The study was carried out on rocky shores along the Portuguese central continental coast, an area delimited in the north and south by long sandy shores. This region incorporates major 3-dimensional variations in coastline orientation and bathymetry (capes, bays and large estuaries) and its oceanography is complex, with recurrent wind stress variation and strong upwelling/downwelling seasonality (Relvas et al. 2007). Initially, and based on the coastal topography and oceanography, we considered 4 main regions along the central west Portuguese coast. We distinguished between the northern and southern Estremadura branches, divided by the Peniche peninsula (Cabo Carvoeiro) and delimited in the south by Cabo Roca (Fig. 1). In Cabo Carvoeiro, there are strong and recurrent wind stress variations, filament formation and separated coastal jets, suggesting the presence of recirculation cells downstream of the capes (Oliveira et al. 2009). Cascais Bay and Arrábida Bay represent important discontinuities along the central Iberian west coast as they are more sheltered from upwelling prevalent winds and under direct influence from 2 major estuaries (the Tagus and the Sado), whose basins drain heavily industrialized areas of Portugal.

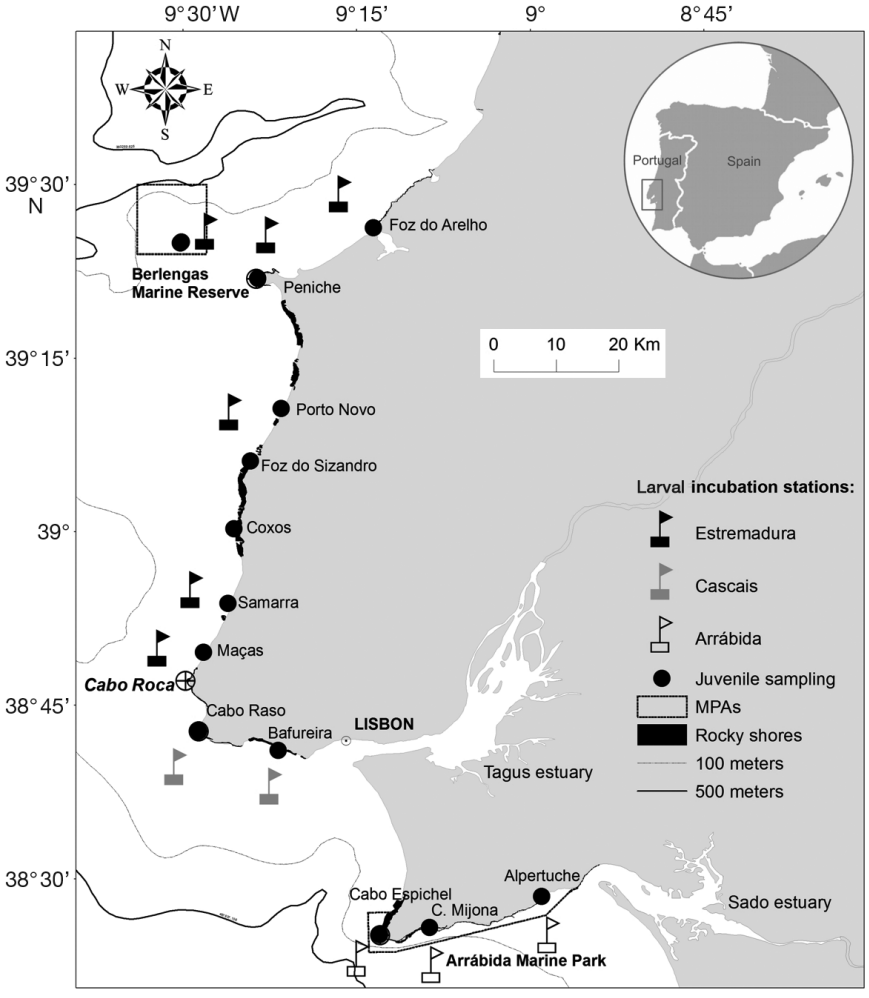

Fig. 1. Larval incubation stations, juvenile sampling sites and location of Marine Protected Areas (MPAs). Estremadura North: Berlengas, Peniche and Foz do Arelho; Estremadura South: Porto Novo, Samarra and Maças; Cascais: Cabo Raso and Bafureira; and Arrábida: Cabo Espichel, Cova da Mijona and Alpertuche. The final regions used to discriminate among natal regions were Estremadura (all moorings located north of Cabo Roca), Cascais and Arrábida. For better visualization purposes, moorings are displayed further offshore here than was actually the case (all moorings deployed at a depth of approx. 15–20 m)

The study area encompasses 2 MPAs included in the Natura 2000 network. In Estremadura, the Berlengas Marine reserve is a coastal archipelago comprising 3 major islands, small islets and reefs. Arrábida Marine Park stretches along 38 km of coastline, from just north of Cabo Espichel to the mouth of the Sado Estuary (Fig. 1).

Mussel spawning and *in situ* larvae incubation

Wild *M. galloprovincialis* adults were collected from the Costa Nova Naval Club pier (Aveiro, Portugal) in early June 2013, and were thoroughly cleaned and stocked dry at 4°C. Spawning was induced the following day by exposing the mussels to cyclic thermal stimulation (20 min in 25°C heated artificial seawater, followed by 20 min in 4°C) and spawning individuals were confined to separate glass jars to collect the gametes independently. Eggs and sperm were filtered through a 125 µm sieve and transferred separately to 250 ml glass cylinders for a quality check under a microscope. A small volume of the sperm solution (<10 ml) was added to the egg suspension and carefully stirred to allow fertilization. After 15 min, the mixture was filtered using a 40 µm sieve to remove excess sperm. Egg concentrations ranged from 350 to 1000 ml^{-1}. All tools, containers and pipettes were non-metallic and subjected to acid leaching (50% v/v MΩ HCl 37%, HCl fuming 37% Emsure grade, Merck) for 24 h, rinsed 3 times in Milli-Q water (Milli-Q 18 MΩ) and dried in a laminar flow chamber.

We followed the Becker et al. (2007) protocol for *in situ* larval incubation and used 25 cm PVC pipe (500 ml inner volume) as larval incubators, with 41 µm Nitex mesh caps on each end. These incubators were washed in advance with Extran MA 03 5% phosphate-free detergent for 1 d, leached in reverse osmosis water for 3 wk (changing the water every 1–3 d) and acid-leached. Approximately 18 000–20 000 larvae (no shell, multi-celled embryos with less than 12 h development) were placed in each incubator and transported inside large buckets filled with artificial seawater to the incubation sites. All incubators were deployed in the water less than 12 h after fertilization. Simultaneously, and to test for incubator effects on larval shell chemical signatures, we also reared larvae in the laboratory: 2 cultures loose in buckets (i.e. no incubators) and 2 cultures inside incubators. The cultures were fed *Isochrysis* sp. every 2 d and allowed to grow for 7 d.

Eleven sites were selected in the central part of the Western Portuguese margin, offshore of a known source of adult mytilid mussel populations. Along the very exposed coast, 3 sites (Foz do Arelho, Peniche and Berlengas) were located north, and 3 sites (Porto

Novo, Samarra and Maças) south of the town of Peniche. Two sites were situated in Cascais (Cabo Raso and Bafureira), and 3 along the Arrábida (Cabo Espichel, Cova da Mijona and Alpertuche) (Fig. 1). On 4 and 5 June 2013, 2 to 3 larval incubators were deployed at each site, at a depth of approximately 3 to 5 m, attached to a polypropylene cable that connected a signalling buoy to a concrete anchor block. Moorings were placed in 15–20 m of water and the buoys were kept submersed (~1.5 m) to minimize theft and conflict with local fishers. One mooring, at Maças, was lost. The incubators were retrieved after 6 d in the water and were immediately filtered using local seawater, stored in acid-washed 120 ml containers and frozen at –20°C. This period allowed for larval shell development under exposure to local physical and chemical environmental conditions.

Early settlers of *M. galloprovincialis* were collected between 23 and 25 July 2013, approximately 43 d after the *in situ* incubation experiment to match the same planktonic development period as the incubated larvae. Three replicates of turf-forming algae were collected at 13 sites (Fig. 1) along the intertidal zone, inshore of the incubator deployment sites. Individuals less than 1.5 mm in length were sorted in acid-washed glass Petri dishes under illuminated magnifying lenses, using Milli-Q water and Teflon-coated extra fine forceps. Samples were frozen (–20°C) in acid-washed Eppendorf vials.

Mytilid larval and juvenile shell extraction and cleaning

All shells prepared for geochemical analysis were processed using non-metallic acid-washed equipment, ultrapure reagents and Milli-Q water (reagents of certified trace metal purity 30% H_2O_2, 99% NaOH and 60% HNO_3 of Suprapur grade, and HCl fuming 37% Emsure grade, Merck). Larval shells were handled under a dissecting microscope, using the tip of a thin paintbrush. Complete shells were selected, separated and carefully placed in Milli-Q water drops. Shells were then transferred into cleaning solution droplets (15% H_2O_2 buffered with 0.1 N NaOH) for 10 min, to remove all organic material, and rinsed 3 times in Milli-Q water, gently swiping the paintbrush in clean Milli-Q water in between relocations. Larval shells were transferred onto a gridded microscope slide that had been pre-coated with a thin layer of resin (Buehler's Epo-Thin™) and were embedded in a small amount of resin, using a fibre paintbrush bristle, to spread it over and around the larval shells, so that they lay flat on the slide. Juvenile shells were prepared using the same methodology, but the valves were manually opened and split using the paintbrush after 15 min in the cleaning solution (heated in 60°C hot water bath). Shell length (larval and juvenile) was measured before embedding the samples onto resin (Buehler's Epo-Thin™)-coated gridded microscope slides. Juvenile shells were positioned with the umbo facing upward.

LA-ICPMS analysis

Concentrations of trace elements in mytilid shells were determined using an Agilent 7700 Inductively Coupled Plasma-Mass Spectrometer (ICP-MS) coupled to a HelEx (Laurin Technic and the Australian National University) laser ablation (LA) system with a 193 nm Compex 110 (Lambda Physik) excimer laser. Random blocks of 18 samples each were run to avoid possible bias due to short-term instrument drift. Each block of samples was bracketed by runs of calibration standards spiked with trace elements (National Institute of Standards and Technology NIST 610 and 612) and a matrix-matched consistency standard MACS-3 USGS (US Geological Survey MACS-3) for estimating external analytical precision (% relative standard deviation, RSD) (Table 1). Prior to each standard and

Table 1. Detection limits (DL), percentages of samples above DL and precision estimates (% relative standard deviation, RSD) for the LA-ICPMS analysis of *Mytilus galloprovincialis* larvae and juvenile shells. DL are based on blank analyses (18 per block of samples) and are expressed in molar ratios relative to mean Ca concentration in a sample. External precision estimates are based on %RSD using standards that most closely approximated the concentration of each element in a sample (MACS-3 used for all elements except for K and U, for which NIST 612 was used)

Element	DL (mol^{-1} Ca)	% above DL	%RSD
Li	10.49227 ($\times10^{-6}$)	27	5.1503
B	0.08156 ($\times10^{-3}$)	71	13.4084
Mg	0.00702 ($\times10^{-3}$)	100	3.1578
P	0.17119 ($\times10^{-3}$)	92	7.452
S	0.96897 ($\times10^{-3}$)	82	7.5643
K	0.09088 ($\times10^{-3}$)	93	12.4534
Mn	2.24422 ($\times10^{-6}$)	59	2.5061
Co	0.55398 ($\times10^{-6}$)	17	6.8978
Cu	1.5772 ($\times10^{-6}$)	85	7.006
Zn	0.00317 ($\times10^{-6}$)	100	7.8005
Sr	0.00412 ($\times10^{-3}$)	100	4.3558
Cd	0.07271 ($\times10^{-6}$)	41	5.6593
Ba	0.00044 ($\times10^{-6}$)	100	3.6053
Ce	0	100	4.5512
Pb	0	100	7.0967
U	0.00003 ($\times10^{-6}$)	100	2.6832

sample analysis, a 30 s blank was acquired to correct for background noise to estimate the limits of detection of the method (Table 1). Both larval and juvenile shell microchemical composition were analysed individually using single-spot laser ablation (single crater; laser beam diameter = 32 µm, laser energy = 60 mJ, laser repetition rate = 5 Hz). Newly recruited juvenile shells were ablated in the umbo region of the early prodissoconch (larval shell). The elements acquired were: ^{7}Li, ^{11}B, ^{24}Mg, ^{31}P, ^{34}S, ^{39}K, ^{43}Ca ^{55}Mn, ^{59}Co, ^{63}Cu, ^{66}Zn, ^{88}Sr, ^{111}Cd, ^{140}Ce, ^{208}Pb and ^{238}U. For the larval samples, we only considered the readings that had at least 60 000 counts of Ca, since many elements were below the detection limit of the method for samples with lower yields. For juvenile samples, and given the small size and orientation of the prodissoconch in the horizontal position of the shell, we restricted the data integration to include only the scans for the first 2 s of sample ablation. This was done to minimize contamination of the natal habitat signature as the laser burned through the early larval shell and into the underlying late-stage larval and juvenile shell (Strasser et al. 2007). This could be a potential problem with larvae that may spend only a short time at their natal location, influenced by strong currents or upwelling events, as is the case for our study area. Data were post-processed to remove any spikes (single scan values greater than 2 times the median of 3 adjacent scans) and smoothed (using a running average of 3 scans) to reduce the noise due to analytical imprecision. Standards and samples were blank subtracted and the abundance of trace elements was standardized to molar ratios relative to calcium, to account for differences in the amount of ablated material.

Environmental data

A daily upwelling index (UI; $m^3\ s^{-1}\ km^{-1}$) at Cabo de Roca was calculated from the 6-hourly data available (from 1 June to 31 July 2013) by the Spanish Institute of Oceanography (Instituto Español de Oceanografía www.indicedeafloramiento.ieo.es). This index is calculated according to Lavín et al. (1991) for the Iberian Peninsula and using sea level pressure of the Meteogalicia WRF atmospheric model (www.meteogalicia.es/modelos). Daily sea surface temperature (SST; °C) was averaged for each region (Estremadura, Cascais and Arrábida) from data provided by the HYCOM model (www.hycom.org) using the same configuration as Nolasco et al. (2013b) with a 3 km resolution. HYCOM is a community ocean model that utilizes generalized vertical coordinates (Bleck 2002). Daily chlorophyll *a* (chl *a*) concentration for each region was averaged from chl *a* (mg m^{-3}) maps derived from MODIS data obtained from the Goddard Space Flight Centre's ocean colour data archive (www.nasa.gov/goddard).

Statistical analysis

We started by analyzing for any incubator effects on trace element concentrations in the larval shells raised at the laboratory using 1-way ANOVA. Data were transformed (log+0.01 for all element ratios except ^{31}P:^{43}Ca, which was 4th-root transformed) in order to meet assumptions of normality and homoscedasticity. Because a significant increase in concentration was found for 10 trace elements in larval shells reared inside incubators, we proportionally subtracted that effect from the signatures of the larvae cultured in the field. We then performed a linear discriminant function analysis (DFA) on the resulting element ratios (X:^{43}Ca) to test the discrimination capability of multi-elemental fingerprints in larval shells among regions (Estremadura North, Estremadura South, Cascais and Arrábida). An analysis on geochemical differences among sites was not possible due to the small sample size at the site level. A forward stepwise analysis was employed to select the elements to build the discriminant functions (F to enter = 1.5) and prior probabilities were computed taking into account group sizes. Reclassification success was evaluated using a jack-knifed classification matrix. A randomization method (White & Ruttenberg 2007) was used to assign p-values to jack-knifed reclassification success estimates, and standardized canonical discriminant function coefficients were evaluated to assess the relative contribution of each trace element in calculating group assignment. One-way ANOVAs followed by post hoc Tukey's tests were performed to test the effect of region on the concentration of the element ratios introduced in the LDA functions. To determine whether our sampling effort was sufficient to capture variability within the 3 regions, based on Simmonds et al. (2014), we carried out linear DFA using Monte Carlo cross-validation over different subsets of the data set (100, 90, 80, 70 and 50% of the data) as implemented in the mlr library (Bischl et al. 2016) of R 3.2.5 (R Core Team 2016, www.r-project.org). For each fraction of the original data set, we performed 1000 iterations where data were randomly selected and misclassification error calculated. The larval shell DFA was then used

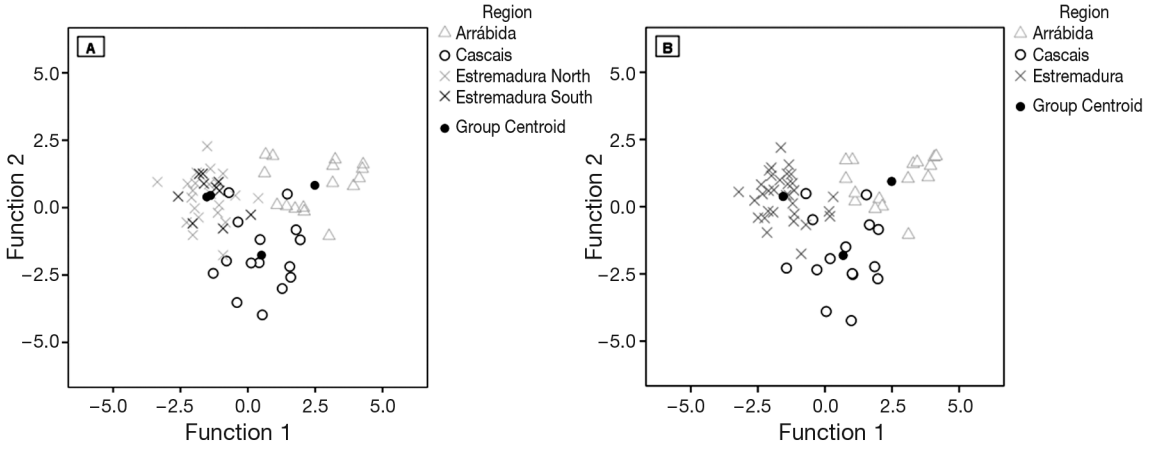

Fig. 2. Canonical score plots of the linear discriminant function analyses (DFA) for incubated larval shells of *Mytilus galloprovincialis* (4–11 June 2013), by regions. Each data point represents 1 shell; regions are represented by a separate symbol and shade. In (A), we used our predefined regions based on local topography and oceanography. Data shown in (B) represent linear DFA using 3 regions

as a training set to assign recruits to natal origin. When assigning recruits to a natal source, DFA assumes all individuals to have originated from one of the 3 regions provided in the training dataset. As we did not sample all potential source populations, we assumed a conservative approach such that any recruit assigned to a specific natal region with a probability of group membership <0.90 had an 'unknown' origin. Finally, we calculated dispersal distance and direction for each successfully assigned individual (dispersal distance ranges were calculated from the collection site to the nearest and furthest point inside the natal region). We considered self-recruits to be all individuals estimated to have settled into the same region in which spawning took place.

RESULTS

Larval incubation and creation of an atlas of natal signatures

In situ mussel larval incubations yielded larval shells formed entirely at known locations, but survival rates inside the incubators were very low (<1%). The small size and fragility of the shells resulted in additional sample loss during shell extraction and cleaning. Sample numbers and mean (±1 SEM) shell length were: Estremadura North n = 21, 115.6 ± 3.8 µm; Estremadura South n = 11, 92.8 ± 3.3 µm; Cascais n = 15, 116.9 ± 5.7 µm; and Arrábida n = 16, 97.8 ± 5.8 µm. The larval shells of M. *galloprovincialis* showed differences in geochemistry that allowed us to separate them using linear DFA. Grouping the incubated larval shells by site resulted in low accuracy of assignment (average of 43.7% of cross-validated cases correctly classified). The assignment accuracy increased at the regional level (Estremadura North, Estremadura South, Cascais and Arrábida regions), with an average of 68.3% of cross-validated cases correctly classified (Fig. 2A, Table 2). However, Estremadura North and Estremadura South regional-specific geochemical signatures showed linear discriminant scatterplots with overlapping group cen-

Table 2. Jack-knife classification success of discriminant function analysis of incubated *Mytilus galloprovincialis* larval shells, with sampling sites grouped into 4 and 3 regions. Correct classifications are in **bold** (average of 68.3% and 79.5% of cross-validated cases correctly classified, when considering 4 and 3 regions, respectively; n = number of individuals)

Region	Predicted group membership (%)			
	Arrábida	Cascais	Estremadura North	Estremadura South
Arrábida (n = 16)	**75.0**	12.5	12.5	0.0
Cascais (n = 15)	20.0	**60.0**	20.0	0.0
Estremadura North (n = 22)	4.5	4.5	**81.8**	9.1
Estremadura South (n = 10)	0.0	20.0	40.0	**40.0**
	Arrábida	Cascais	Estremadura	
Arrábida (n = 16)	**75.0**	12.5	12.5	
Cascais (n = 15)	20.0	**60.0**	20.0	
Estremadura (n = 32)	0.0	9.4	**90.6**	

troids (Fig. 2A, functions 1 and 2 of group centroids = −1.5, 0.4 and −1.4 and 0.4, respectively) with low (40%) cross-validated classification success in the Estremadura South region (Table 2). Therefore we decided to combine both locations into one single open coast region (Estremadura) and rerun the linear DFA (Fig. 2B). The resulting cross-validated classification success increased to 79.5% (Table 2), significantly higher than the 33.0% expected by chance alone (p = 0.0002; White & Ruttenberg 2007). All the subsequent analyses were performed using 3 natal source regions: Estremadura, Cascais and Arrábida.

Classification accuracy was highest for larvae incubated in the Estremadura region (90.6%) and lowest for Cascais (60.0%; Table 2). Eight trace elements entered the model (B, P, Co, Cu, Zn, Ce, Pb and U) and the first canonical function explained 73% of total variance, with Pb, Zn, B and P with positive loadings and Cu, Co, Ce and U with negative loadings (Table 3). The second canonical function explained the remaining 27% of total variance, with Zn and Co loading negatively. Arrábida and Estremadura were separated mostly by the first function, with positive values for Arrábida and negative values for Estremadura, indicating higher concentrations of Pb and P in Arrábida. The second function separated Cascais from the other 2 regions, with higher values of Zn in this region. Univariate ANOVA comparing ratios to calcium for the 8 elements used to discriminate larval shells among regions resulted in significant differences in 4 elements (Pb:Ca, $F = 24.463$, p = 0.00001; Zn:Ca, $F = 11.501$, p = 0.000059; U:Ca, $F = 0.961$, p = 0.000086; Ce:Ca, $F = 3.878$, p = 0.026065; Table 4). Larval shells incubated in Cascais had significantly higher concentrations of Zn and lower concentrations of Ce compared with the other 2 regions; for Pb concentrations, Arrábida>Cascais>Estremadura, and for U concentrations, Estremadura=Arrábida>Cascais (Fig. 3). Mean misclassification error to the region level (3 regions: Arrábida, Cascais and Estremadura) derived from the full model and from the cross-validation with 10, 20, 30 and 50% of the data withheld were then compared using an ANOVA ($F = 19.71$, $p < 0.001$). Tukey's HSD post hoc tests confirmed no significant differences in misclassification error between the full model and those subsets that included at least 80% of the data. The consistency detected on classification success among those subsets confirmed our capability to detect distinctive signatures for each region and that we had sufficient sampling effort to account for variability within each region.

Table 3. Standardized canonical discriminant function coefficients corresponding to the canonical score plot shown in Fig. 2B. Percentages of variance and canonical correlation coefficients for each function are also shown

Molar ratio	Function 1	Function 2
$^{11}B:^{43}Ca$	0.484	0.353
$^{31}P:^{43}Ca$	0.708	0.486
$^{59}Co:^{43}Ca$	−0.558	−0.323
$^{63}Cu:^{43}Ca$	−0.735	0.088
$^{66}Zn:^{43}Ca$	0.209	−1.024
$^{140}Ce:^{43}Ca$	−0.246	0.254
$^{208}Pb:^{43}Ca$	1.271	0.268
$^{238}U:^{43}Ca$	−0.644	0.342
% variance	73	27
Canonical correlation coefficient	0.868	0.729

Table 4. Results from univariate ANOVAs of the effect of region (Estremadura, Cascais and Arrábida) on trace element concentrations in larval shells of *Mytilus galloprovincialis*. Only trace elements that entered the linear discriminant function model were included in this analysis. **Bold** values indicate significant effects at the 5% significance level. Post hoc pairwise com-parisons using Tukey's tests are shown in Fig. 3

Source of variation	df	SS	MS	F_s	p
$^{208}Pb:^{43}Ca$					
Region	2	5.513	2.756	24.463	**0.00001**
Error	60	6.250	0.104		
Total	62	11.763			
$^{66}Zn:^{43}Ca$					
Region	2	4.319	2.160	11.501	**0.000059**
Error	60	11.267	0.188		
Total	62	15.586			
$^{238}U:^{43}Ca$					
Region	2	1.922	10.980	0.961	**0.000086**
Error	60	5.252	0.104		
Total	62	7.175			
$^{140}Ce:^{43}Ca$					
Region	2	1.244	0.622	3.878	**0.026065**
Error	60	9.622	0.160		
Total	62	10.866			
$^{11}B:^{43}Ca$					
Region	2	0.161	0.080	2.343	0.105
Error	60	2.056	0.034		
Total	62	2.216			
$^{31}P:^{43}Ca$					
Region	2	0.241	0.136	1.766	0.180
Error	60	4.612	0.077		
Total	62	4.883			
$^{59}Co:^{43}Ca$					
Region	2	0.216	0.108	1.062	0.352
Error	60	6.096	0.102		
Total	62	6.312			
$^{63}Cu:^{43}Ca$					
Region	2	0.380	0.190	1.062	0.352
Error	60	10.732	0.179		
Total	62	11.111			

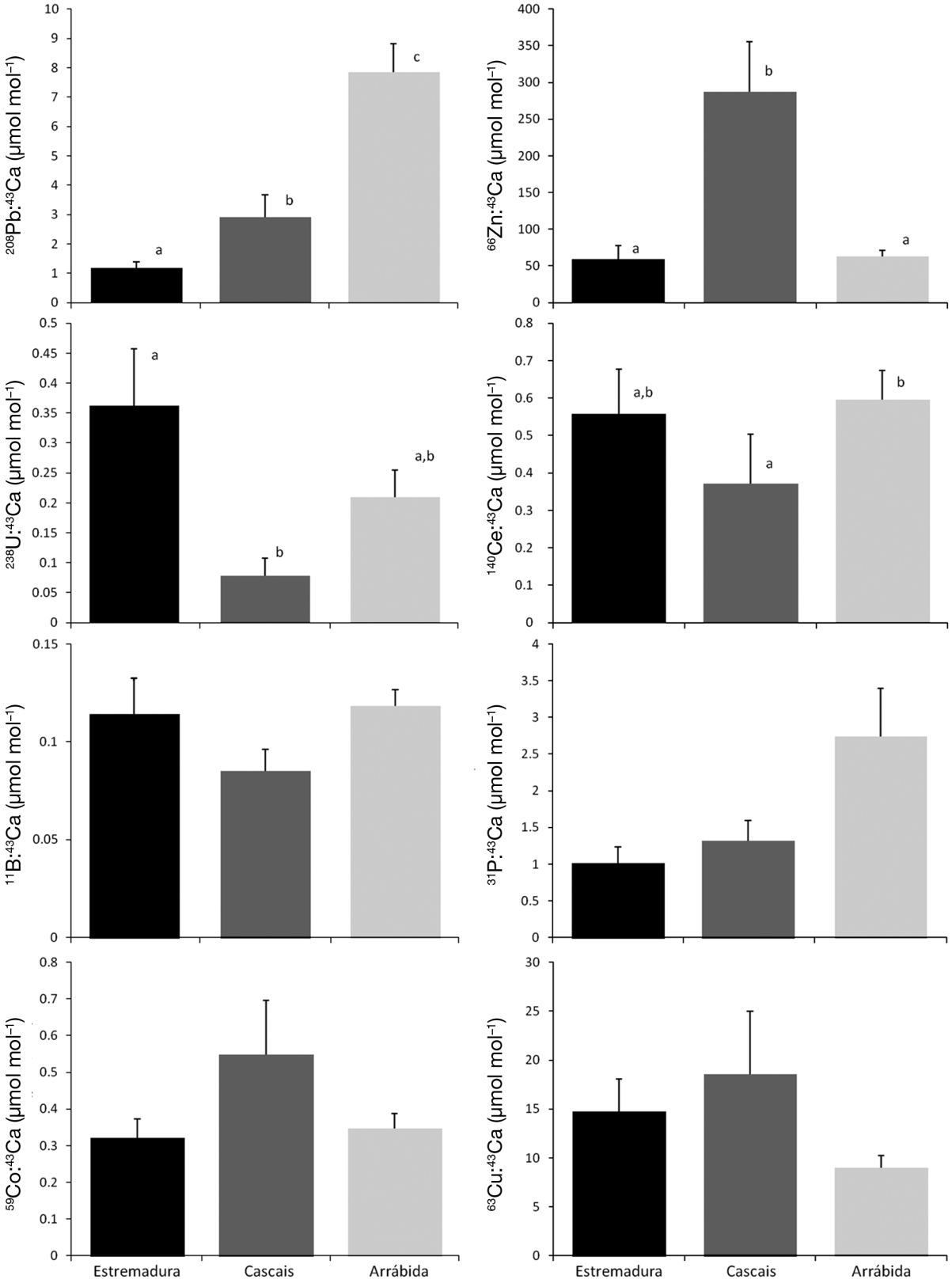

Fig. 3. Ratios to calcium for the 8 elements used to discriminate larval shells of *M. galloprovincialis* from the regions Estremadura, Cascais and Arrábida. Bars represent regional means ±1 SE. Different letters above bars indicate significant ($p < 0.05$) differences according to Tukey's post hoc tests

Establishment of natal origin of juveniles

A total of 128 recent settlers of *M. galloprovincialis* were collected in the Estremadura region at 8 sites (mean ± 1 SEM length, 462.7 ± 31.18 µm), 30 in Cascais at 2 sites (833.3 ± 172.35 µm), and 43 individuals in Arrábida at 3 sites (549.57 ± 30.37 µm). The collection occurred approximately 42 d after the incubation period. The small size of the individuals assembled (534.23 ± 49.01 µm) indicates that settlement had occurred in the preceding 2–3 wk. With a larval duration of approximately 3–4 wk for this species, at the temperatures recorded during the study, the larval incubation period matches the early stages of planktonic larval development for these recruits. Out of 201 juvenile mussels, 81 (40.3%) were classified as of unknown origin (probability of group membership <0.90), most of them collected from Estremadura (72.8%). When 'relaxing' our criteria for successful recruit assignment based on the posterior probabilities in the DFA, the overall percentage of individuals from 'unknown origin' drops from 40.3% (<0.90) to 24.4% (<0.75) and to 5% (<0.5). In all 3 scenarios, however, the general pattern in larval dispersal distance and direction remains the same. For this reason, and because we want to account for the inherent uncertainty in the atlas of natal signatures, we have presented the most conservative approach in larval assignment and discuss the likely origins of unknown individuals based on local oceanographic and topographic characteristics. Within a region, the natal origin of the recruits collected was variable, with recruits in the Estremadura region showing the greatest diversity in terms of natal sources (Fig. 4), suggesting high heterogeneity in the local hydrodynamics. Recruits collected in the bays of Cascais and Arrábida primarily fall under the domain of Arrábida natal signature, accentuating the high self-recruitment within this bay, high larval export from Arrábida and no self-recruitment within Cascais Bay for this period.

We found evidence for mussels in Estremadura to have originated from Arrábida, with recruits collected as far north as Baleal and Berlengas estimated to have dispersed more than 100 km north (Fig. 5). Some recruits collected in Estremadura originated from Cascais (9%), but self-recruitment was also detected

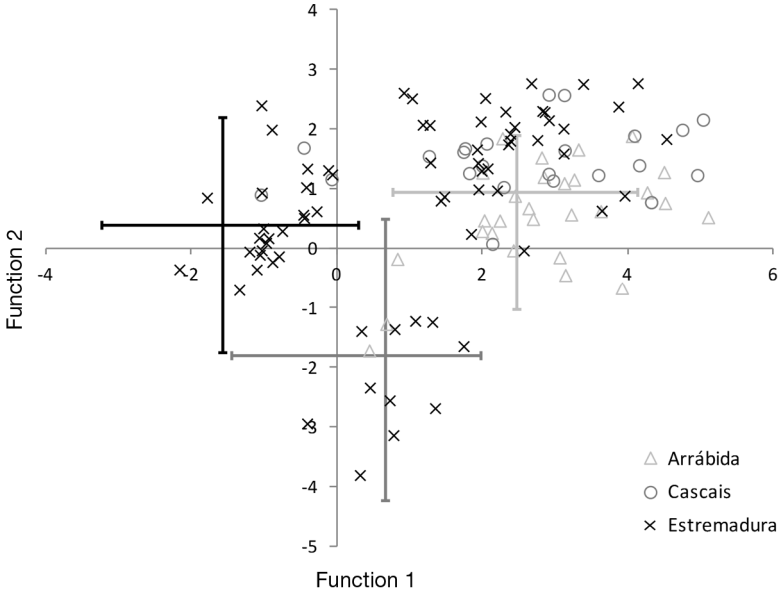

Fig. 4. Canonical score plot of the individual recruits according to the discriminant analysis based on larval shell elemental signature. Symbols indicate sampling regions for recruits. Lines represent average larval scores (centroid) and extent (maximum and minimum values) for each region, following the shade code: light grey, dark grey and black for Arrábida, Cascais and Estremadura, respectively. Recruits that fell under the 90% confidence interval for assignment are not shown

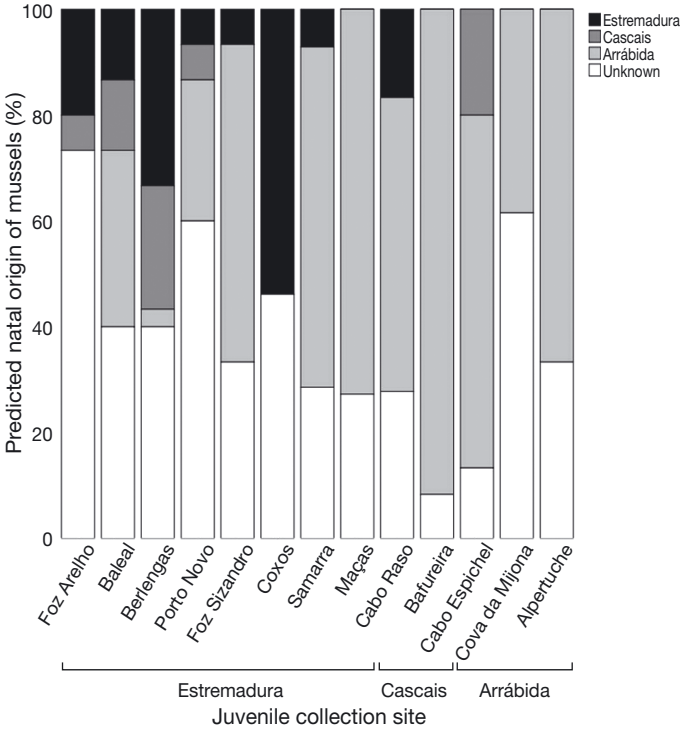

Fig. 5. Predicted natal origins of juvenile mussels. The *x*-axis represents collection sites of juvenile mussels (early settlers), grouped by main regions, and the shading of the bars symbolize predicted natal origins determined using regional larval shell DFA functions as a training set. Sites are organized from north (left) to south (right). See Fig. 1 for a site map

within the region (19% of juveniles collected in the Estremadura region originated in that region) (Fig. 6). Cascais showed no self-recruitment and appeared to be the region that contributed the least in terms of larval export to other regions. Interestingly, 70% of all recruits collected in Cascais came from Arrábida Bay (which is an MPA). The Arrábida MPA showed the greatest contribution as a source population, and high levels of self-recruitment (58%), with only few recruits originating from Cascais (5%) and none from the most northern region, Estremadura (Fig. 6). Natal origins of recruits in the Berlengas MPA were the most diverse, with little connectivity to the Arrábida MPA. In terms of dispersal direction, 55.4% of the reassigned recruits originated from southern natal sources, and only 4.1% were supplied from northern locations, which clearly indicates a northward dispersion pattern (Fig. 7). Regarding distances, most of the recruits analyzed here were estimated to have dispersed less than 50 km away from their natal source, with maximum dispersal ranges of about 120 km.

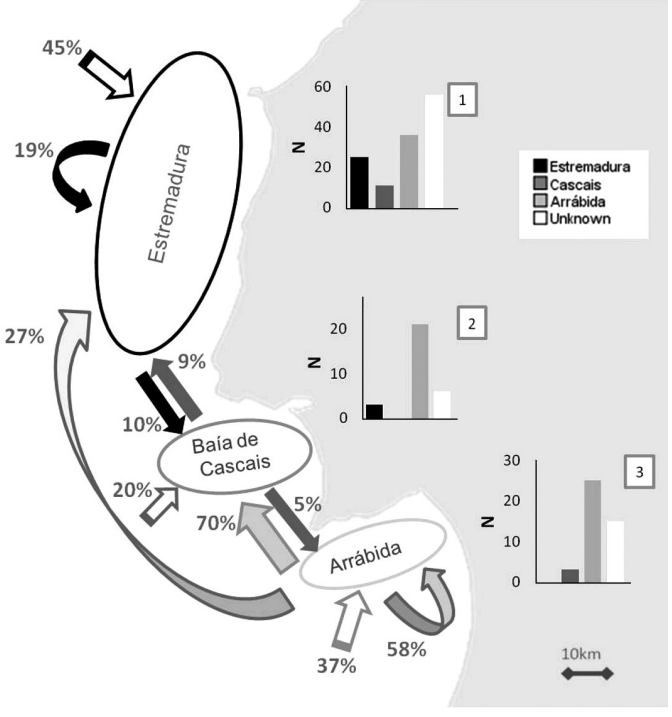

Fig. 6. Predicted dispersal pathways of *Mytilus galloprovincialis* larvae among the 3 regions along the central west coast of Portugal, from mid-June to mid-July 2013. Color and width of arrows represent the natal origin and percentage, respectively of recruits that originated from the region at the base of the arrow. White arrows indicate unknown origin. Bar graphs 1, 2 and 3 correspond to the number of juveniles collected (N, by region) and predicted natal origins (by region), for Estremadura, Cascais and Arrábida, respectively

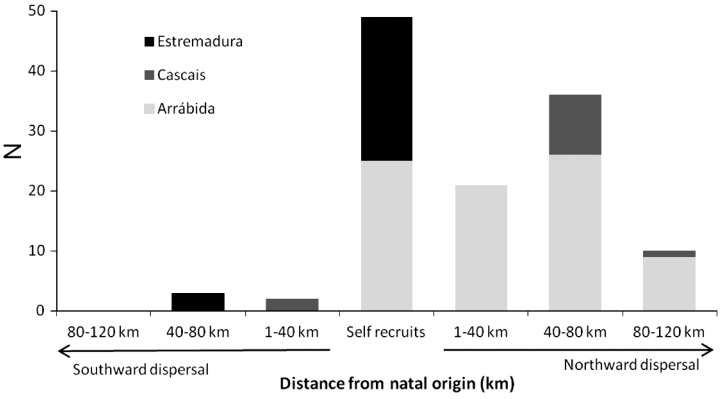

Fig. 7. Predicted dispersal direction and distance from natal source (Estremadura, Cascais, Arrábida; km) of successfully assigned *Mytilus galloprovincialis* recruits (n = 121), from mid-June to mid-July 2013. N, number of recruits. Self-recruits are individuals estimated to have settled into the same region where spawning took place

Environmental data

The daily UI series (Fig. 8) from June and July 2013 at Cabo da Roca showed a strong upwelling event from 15 June until 3 July, followed by an extensive relaxation period which lasted until 24 July. This long relaxation period (3 wk) is unusual for this season, which is typically characterized by prevailing northerly winds (Relvas et al. 2007). An abrupt SST warming took place immediately after the upwelling maximum on 23 June, rising from average values oscillating around 14.5°C on 21 June to average values of 18.8°C on 11 July, and stayed high until the end of July. Daily chl-*a* concentrations increased from around 2 mg m^{-3} before the upwelling event to between 6 and 8 mg m^{-3} immediately after the upwelling maximum, stayed high during the event and decreased again to around 2 mg m^{-3} during the relaxation event. These temporal patterns are consistent with a northward advection of a warm water mass starting around 25 June, approximately 15 d after the larval incubation trial, which continued until the sampling of the recruits from 23 to 25 July.

DISCUSSION

Larval shell geochemical signatures

In this study, we provide further evidence that the geochemical composition of *Mytilus galloprovincialis* larval shells can provide valuable information in the form of environmental and natal markers which are crucial in tracking larval dispersal pathways. *M. gal-*

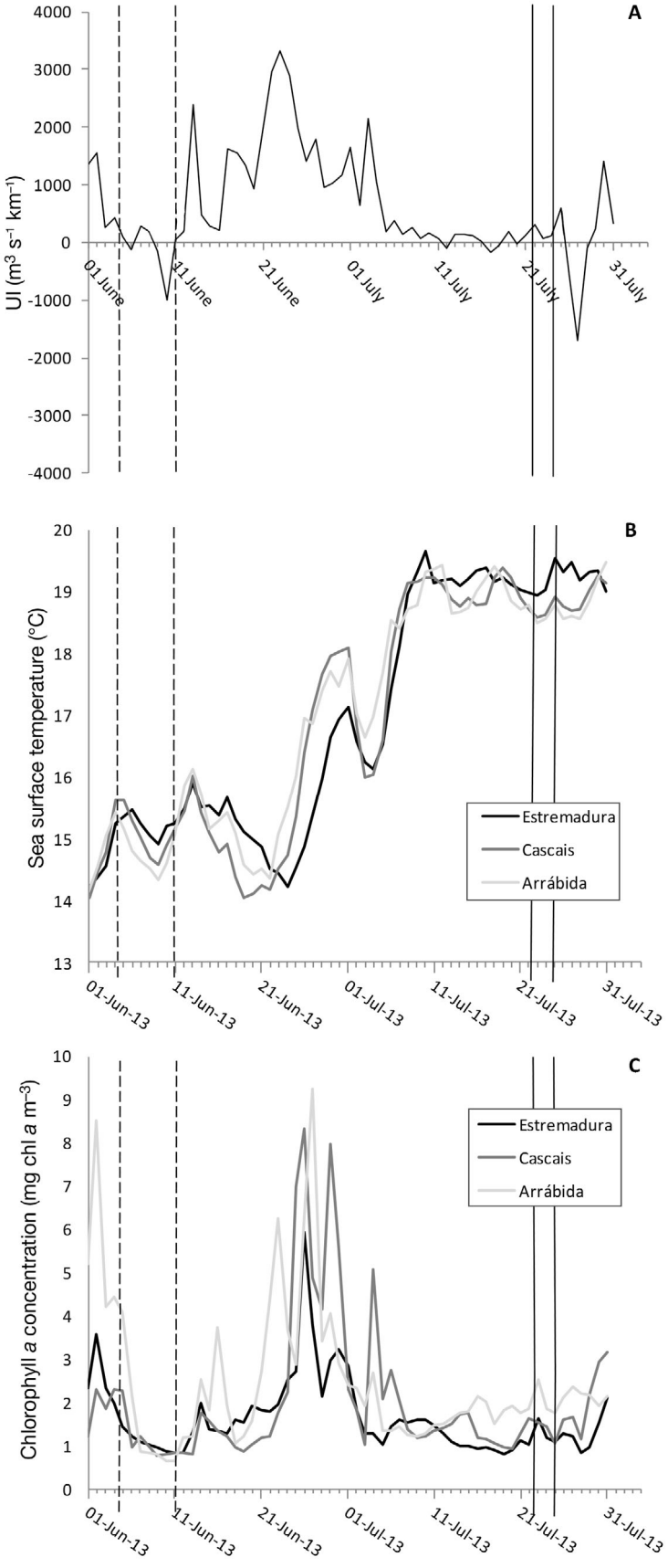

Fig. 8. Daily time series of (A) the upwelling index (UI) estimated for Cabo de Roca, (B) sea surface temperature (SST; °C) and (C) chlorophyll *a* concentration averaged separately for each region, during June and July 2013. In (A), negative values indicate downwelling. Larval incubation and recruit sampling periods are indicated by vertical dashed and solid lines, respectively

loprovincialis larvae reared at different sites along the central Portuguese west coast showed distinctive trace elemental signatures at the regional level, discriminating between the open coast and 2 large embayments exposed to industrialized estuaries. Distinctive elemental signatures in the biogenic carbonate from invertebrate larvae between open coast and bay habitats have been described previously (Becker et al. 2005, Carson 2010, Fodrie et al. 2011). Trace element incorporation in biominerals can be influenced by a variety of factors, such as elemental concentrations in local seawater, and seawater temperature, salinity and pH (Campana 1999, Chittaro et al. 2006, Levin 2006). During the incubation experiment, however, SSTs and salinities from all sites were very similar across the studied area (temperature ranged from 14.75 to 15.81°C, and salinity varied between 35.93 and 36.09). Although the incorporation mechanisms involved in the site-specific trace elemental composition in larval calcified structures are still uncertain for most elements, this knowledge is not required to successfully apply the technique for tracking natal origins (Gillanders 2002, Zacherl 2005, Becker et al. 2007, Carson 2010, Cook et al. 2014). In our study, zinc (Zn), lead (Pb) and uranium (U) concentrations on mytilid larval shells were the main variables responsible for discriminating regional signatures. These elements are amongst the group of useful elements (Mg, Cr, Mn, Co, Cu, Zn, Sr, Cs, Ba, Pb and U) reviewed by Carson et al. (2013) in southern California in which the variation in the environment is usually reflected in teleost fish otoliths, bivalve shells and crustacean larvae. Both estuaries in our study area (the Tagus and the Sado) have been extensively documented as having increased anthropogenic trace metal concentrations (from urban wastewater, agricultural runoff and industrial effluents) in adjacent waters, suspended particulate matter, surface sediments and sediment cores (Caeiro et al. 2005, Costa et al. 2011, Santos-Echeandía et al. 2012). Our results

showed that larvae reared inside Cascais Bay had higher concentrations of Zn in the shell. This is consistent with high trace metal concentrations in the surface waters and sediments in the Tagus Estuary due to the effluents from chemical, steelwork and shipbuilding industries (Cotté-Krief et al. 2000). Arrábida Bay larval shells contained the highest concentrations of Pb. Richter et al. (2009) also found anthropogenic Pb stable isotope signatures in sediment cores of the Setúbal-Lisbon canyons system, consistent with fly ash inputs from waste incinerators, and an efficient transfer from the river discharge to the adjacent shelf. Pb has been reported as an effective marker in mussel shells in relation to polluted bays (San Diego Bay; Becker et al. 2005). Pb incorporation in the shell is frequently well correlated with water Pb concentration (Carson et al. 2010, Fodrie et al. 2011), and it is one of the elements showing less temporal variability in the open coast (Fodrie et al. 2011).

Along the exposed coast of Estremadura, larval shells showed significantly higher concentrations of U. Recently, the incorporation of U in biogenically precipitated carbonates has received some attention as a potential acidification geochemical proxy in foraminifera, corals and mollusk larval shells (reviewed in Levin et al. 2015). To probe for a geochemical proxy that reflects pH exposure in mussel larval shells, Frieder et al. (2014) cultured *M. galloprovincialis* in the laboratory across a range in pH and temperature, and confirmed that U/Ca incorporation reflected mean pH conditions in the water, following a strong negative correlation, regardless of larval shell size, oxygen concentration or temperature. Additionally, the authors successfully applied that proxy to larvae reared along a spatial gradient in upwelling in southern California, detecting higher U/Ca ratios in larval shells reared in colder, low pH waters. Similarly, in the exposed Estremadura region, CO_2-enriched and low-pH upwelled waters might explain the higher U/Ca when compared with the contiguous and more protected bays of Cascais and Arrábida. However, we were unable to find pH values for this region and period to test for this hypothesis.

Although we found spatially distinct multi-elemental signatures, we do not know whether the signatures are temporally stable. However, studies have suggested that trace element compositions within newly recruited bivalve shells (Becker et al. 2005) and larval shells (Cathey et al. 2014) can be relatively stable over weekly to monthly time scales. Even when signatures are temporally variable, spatial discrimination using bivalve shell chemistry is still often possible (Fodrie et al. 2011, Carson et al. 2013). The elements responsible for regional discrimination in this study are likely associated with consistent environmental differences among locations (i.e. strong upwelling exposed coasts versus bays influenced by urbanized estuaries). Nonetheless, the complexity of the shoreline, variable ocean circulation and dynamic nature of atmospheric and hydrologic pollution inputs actively influence and modify seawater geochemistry in coastal and estuarine systems (Swearer et al. 2003, Thorrold et al. 2007, Miller et al. 2013). Also, more studies are needed to fully understand how the material and environment inside artificial incubators can indeed interfere with the element uptake into the larval shell carbonate matrix. The potentially different elemental signature of incubator versus wild shells could hinder the recruit's assignment to natal origins. Further work should consider the use of diverse incubators, of different sizes and materials, and different larval densities and parenting pools, in order to improve *in situ* rearing settings and to advance our understanding of the formation of geochemical signatures under 'caging conditions'. Nevertheless, we are confident that our results from the larval housing units were able to record regional variation in source signatures between the open coast and 2 urbanized bays, where the environmental factors have prevailed over any regional maternal effects, and any effect due to leaching of elements from the incubators. This work represents a momentary and potentially transitory atlas of chemical fingerprints; a 'snapshot' of the local physical, chemical and oceanographic characteristics between June and July 2013.

Dispersal pathways versus local oceanography

When we assigned early mussel settlers to source populations across 120 km of coastline along the central west coast of Portugal, we were able to quantify natal origin and dispersal trajectory for 59.7% of the collected settlers. Within a region, the natal origin of the recruits collected was variable, mainly for the northern Estremadura region, where the number of 'unknown origins' was also greater, which might suggest high heterogeneity in the local hydrodynamics in this open coastal setting. There were, however, 2 major sources of uncertainty included in the model: recruits that originated from outside of our study region (even though our sampling was delimited by long, sandy shorelines, an unsuitable habitat for

mussels) and recruits that originated from within our study region, but where the signature from the source location was less consistent. For these reasons, we followed a conservative approach and only assumed successful recruit assignment when the probability (posterior probabilities in DFA) was >0.9.

Bivalves have been described as potentially long-distance dispersers, with estimated dispersal distances reaching to hundreds of kilometers (Bayne 1976). McQuaid & Phillips (2000) calculated that the majority of recruits of *M. galloprovincialis* in South Africa settled <5 km from the parent population. Previous studies using genetics (Kinlan & Gaines 2003), genetics and physical oceanography (Gilg & Hilbish 2003), trace elemental fingerprinting (Becker et al. 2007) and spatial geostatistical analysis (Smith et al. 2009) have also documented moderate dispersal distances (20–40 km) among open coast mussel populations. López-Duarte et al. (2012) also reported alongshore dispersal distances of approximately 35 km for *Mytilus californianus* and 37 km for *M. galloprovincialis* between generalized regions of origin and destination, in southern California. Accordingly, and even though the present study revealed larval exchange among regions separated by more than 100 km, for most of the recruits analyzed the dispersal distance was estimated to be less than 50 km away from the natal source. However, the dispersal range analysis was constrained by the regional resolution of the natal signatures because geographical distances within and amongst natal regions diverge. Nevertheless, this illustrates how far larvae can disperse under the local upwelling/relaxation events.

In terms of dispersal direction, we observed an overall northward dispersal. The Estremadura region, which is much larger than the other 2 regions and has the most adult mussel habitat, contributed only 1.5% to other regions. This northward overall dispersal direction was unexpected because spring and summer periods are characterized by upwelling favorable winds, resulting in southward ocean surface circulation over most of the shelf (as reviewed by Relvas et al. 2007). However, wind-stress reversals and upwelling relaxation events are common along the west Iberian coast at short temporal scales (days), affecting nearshore circulation (Relvas & Barton 2005, Oliveira et al. 2009). Upwelling relaxation events are well described along the eastern boundary of upwelling systems. These events, where the wind forces relax after a coastal upwelling event, have been associated with an increase in nearshore along-shelf poleward flow reversals in California (Melton et al. 2009, Send & Nam 2012) and Chile (Narváez et al. 2006). The UI, recorded in the region during June–July 2013, revealed the presence of an upwelling event followed by an extended upwelling relaxation period, with a sharp increase in SST and a decrease in chl-*a* concentration. Thus, it is possible that the newly formed mussel larvae were initially pulled southward (as a results of the upwelling event), but were then transported northward along the coast in July. Based on a multi-year observational study, Sordo et al. (2001) reported that, upon cessation of upwelling events, a northward flow progressed inshore along the Western Iberian northern margin, causing a narrow band of warm water against the coast. Also, Oliveira et al. (2009), using satellite images and numerical simulations of SST and chl-*a*, reported a rapid onset of coastal counter currents along the inshore zone during upwelling relaxation, with northward flow of oligotrophic waters from Arrábida Bay and occupying part of Cascais Bay. Accordingly, 70% of the recruits we collected in Cascais were supplied by the Arrábida MPA. We found no evidence for self-recruitment in Cascais Bay. The hydrodynamics in this bay are strongly influenced by the Tagus Estuary, one of the largest in Europe, whose plume can be advected offshore during upwelling favorable winds, and pushed back northward along the Estremadura coast during relaxation periods (Vaz et al. 2009).

Implications for management and future directions

Quantifying connectivity among coastal populations and identifying critical habitats to the replenishment of adult populations is crucial for assessing current spatial management approaches and setting the scale for future integrated management plans. Different methods to derive connectivity estimates differ in their specific objectives and/or temporal resolution, varying from integrative to snapshot assessments. Long-term modeling studies have shown that larval connectivity is inherently a stochastic process varying as a function of different biological and physical processes (Siegel et al. 2008). Although the present study derived connectivity estimates from a snapshot approach, such empirically derived metrics are crucial to validate the predictions of coastal connectivity and resource dynamics from larger-scale modeling efforts (Werner et al. 2007).

The Arrábida MPA management plan approved in 2005 imposed prohibition of trawling, dredging and bivalve harvesting, to preserve its role as a nursery for many marine species contributing to the sustain-

ability of the local fishing resources (Cunha et al. 2014). Our results showed that this MPA was the main source population supplying larvae to the other 2 regions, even though connectivity with Berlengas MPA was very limited. The Arrábida MPA also contributed 70% of the recruits collected in Cascais and revealed 58% of self-recruitment within its bay, suggesting that it may be a retention zone for locally spawned larvae. Other studies in the Arrábida MPA have also shown that fish larvae (namely reef-associated species belonging to the families Gobiidae, Tripterygiidae, Labridae and Sparidae) can complete their entire planktonic phase in the vicinity of the adult habitats (Borges et al. 2007). Interestingly, a study of the gene flow of *Perna perna* in South Africa (Nicastro et al. 2008) showed that coastal topography strongly affected larval dispersal and population genetic structure, with bays acting as source populations. However, different reproductive seasons (spring and fall) along with changes in upwelling intensity might result in different dispersal trajectories for mytilid species (Carson et al. 2010).

Self-recruitment and connectivity via larval dispersal have been documented by several authors in the assessment of MPAs: using hydrodynamic (Roberts 1997), biophysical (Cowen et al. 2006) and spatial metapopulation models (White et al. 2010), genetics (Palumbi 2004), dispersal distances (Shanks et al. 2003), parental analysis (Planes et al. 2009) and, more recently, elemental fingerprinting (Di Franco et al. 2012, Cook et al. 2014). Here, we provide evidence for high self-recruitment within the Arrábida MPA for mytilid larvae but limited connectivity with the Berlengas MPA during an upwelling relaxation event. Our results give further emphasis on the need to incorporate dispersal pathways and variability in the local oceanographic setting when developing management plans regarding MPA placement and size.

Recently, Burgess et al. (2014) underlined the significance of local retention (the fraction of offspring produced by a population that also recruits into that population) rather than self-recruitment for the dynamics and persistence of spatially structured populations within MPA networks. In this sense, larval dispersal patterns require knowledge of larval production rates to more accurately evaluate population dynamics and metapopulation persistence. Our next goal is to integrate and combine our results with numerical models of ocean circulation and population dynamic models, in order to have a more complete picture of what drives mytilid population dynamics and persistence in and around a network of MPAs, over larger temporal and spatial scales. Such direct measures of demographic connectivity can be a powerful tool for field practitioners and policy makers in refining monitoring programs and reassessing the configuration of current reserves to deal with the contemporary issue of MPA network ecological coherence along complex topographic and oceanographic coastlines.

Acknowledgements. The authors thank the following individuals and institutions for support and logistic assistance during fieldwork. Maria de Jesus Fernandes, Director of the Departamento de Conservação da Natureza e Florestas de Lisboa e Vale do Tejo of the Instituto de Conservação da Natureza e Florestas, issued sampling permits and provided access to facilities of the Reserva Natural das Berlengas (RNB) and the Parque Natural da Arrábida (PNA). Licenses for rocky shore sampling outside the protected areas were provided by the Agência Nacional do Ambiente. Paulo Crisóstomo, Eduardo Mourato, Tiago Menino, Filipe Correia, Lurdes Morais, Sandra Garrido (RNB), Miguel Henriques, Carlos Silva, Dionisio, Alda Silva, Mafalda Anjo (PNA), Cláudia Moreira and Ana Margarida Gama (Centro Interdisciplinar de Investigação Marinha e Ambiental, Universidade do Porto) provided support during fieldwork. Prof. Sérgio Leandro (Escola Superior de Turismo e Tecnologia do Mar, Peniche) and Prof. Teresa Cruz (Laboratório de Ciências do Mar, Universidade de Évora) provided access to their laboratories. We also thank the 3 anonymous reviewers whose comments greatly improved this manuscript. This study is part of the 'LarvalSources - Assessing the ecological performance of marine protected area networks' research project, funded by Fundação para a Ciência e Tecnologia FCT (PTDC/BIA-BIC/120483/2010). Financial support was allocated by FCT under the COMPETE Programme, which includes components from the European Regional Development Fund and from the Ministério da Ciência, Tecnologia e Ensino Superior. R.A. was supported by FCT (BI/CESAM/PTDC/BIA-BIC/120483/2010). L.P. was supported by a postdoctoral fellowship from Xunta de Galicia, Spain (POS-A/2012/189). I.G.'s PhD work was supported by a MARES grant. MARES is an Erasmus Mundus Joint Doctorate programme coordinated by Ghent University (FPA 2011-0016).

LITERATURE CITED

Adams TP, Aleynik D, Burrows MT (2014) Larval dispersal of intertidal organisms and the influence of coastline geography. Ecography 37:698–710

Ardron JA (2008) The challenge of assessing whether the OSPAR network of marine protected areas is ecologically coherent. Hydrobiologia 606:45–53

Bayne BL (1976) Marine mussels, their ecology and physiology. Cambridge University Press, Cambridge

Becker BJ, Fodrie JF, Mcmillan PA, Levin LA (2005) Spatial and temporal variation in trace elemental fingerprints of mytilid mussel shells: a precursor to invertebrate larval tracking. Limnol Oceanogr 50:48–61

Becker BJ, Levin LA, Fodrie FJ, McMillan PA (2007) Complex larval connectivity patterns among marine invertebrate populations. Proc Natl Acad Sci USA 104:3267–3272

Bischl B, Lang M, Richter J, Bossek J and others (2016) mlr: machine learning in R. R package version 2.8. https://CRAN.R-project.org/package=mlr

Bleck R (2002) An oceanic general circulation model framed in hybrid isopycnic-Cartesian coordinates. Ocean Model 4:55–88

Borges R, Beldade R, Gonçalves EJ (2007) Vertical structure of very nearshore larval fish assemblages in a temperate rocky coast. Mar Biol 151:1349–1363

Börner N, De Baere B, Yang Q, Jochum KP, Frenzel P, Andreae MO, Schwalb A (2013) Ostracod shell chemistry as proxy for paleoenvironmental change. Quat Int 313–314:17–37

Borthagaray AI, Carranza A (2007) Mussels as ecosystem engineers: their contribution to species richness in a rocky littoral community. Acta Oecol 31:243–250

Burgess SC, Nickols KJ, Griesemer CD, Barnett LAK and others (2014) Beyond connectivity: how empirical methods can quantify population persistence to improve marine protected-area design. Ecol Appl 24:257–270

Caeiro S, Costa MH, Ramos TB, Fernandes F and others (2005) Assessing heavy metal contamination in Sado Estuary sediment: an index analysis approach. Ecol Indic 5:151–169

Campana SE (1999) Chemistry and composition of fish otoliths: pathways, mechanisms and applications. Mar Ecol Prog Ser 188:263–297

Campana SE, Thorrold SR (2001) Otoliths, increments, and elements: keys to a comprehensive understanding of fish populations? Can J Fish Aquat Sci 58:30–38

Carson HS (2010) Population connectivity of the Olympia oyster in southern California. Limnol Oceanogr 55: 134–148

Carson HS, López-Duarte PC, Rasmussen L, Wang D, Levin LA (2010) Reproductive timing alters population connectivity in marine metapopulations. Curr Biol 20:1926–1931

Carson HS, López-Duarte PC, Cook GS, Fodrie FJ, Becker BJ, Dibacco C, Levin LA (2013) Temporal, spatial, and interspecific variation in geochemical signatures within fish otoliths, bivalve larval shells, and crustacean larvae. Mar Ecol Prog Ser 473:133–148

Cathey AM, Miller NR, Kimmel DG (2014) Spatiotemporal stability of trace and minor elemental signatures in early larval shell of the northern quahog (hard clam) *Mercenaria mercenaria*. J Shellfish Res 33:247–255

Chicharo MA, Chicharo MZ (2000) Estimation of the life history parameters of *Mytilus galloprovincialis* (Lamarck) larvae in a coastal lagoon (Ria Formosa, south Portugal). J Exp Mar Biol Ecol 243:81–94

Chittaro PM, Hogan JD (2013) Patterns of connectivity among populations of a coral reef fish. Coral Reefs 32: 341–354

Chittaro PM, Usseglio P, Fryer BJ, Sale PF (2006) Spatial variation in otolith chemistry of *Lutjanus apodus* at Turneffe Atoll, Belize. Estuar Coast Shelf Sci 67:673–680

Cook GS, Parnell PE, Levin LA (2014) Population connectivity shifts at high frequency within an open-coast marine protected area network. PLoS One 9:e103654

Costa AM, Mil-Homens M, Lebreiro SM, Richter TO and others (2011) Origin and transport of trace metals deposited in the canyons off Lisboa and adjacent slopes (Portuguese Margin) in the last century. Mar Geol 282:169–177

Cotté-Krief MH, Guieu C, Thomas AJ, Martin J (2000) Sources of Cd, Cu, Ni and Zn in Portuguese coastal waters. Mar Chem 71:199–214

Cowen RK, Paris CB, Srinivasan A (2006) Scaling of connectivity in marine populations. Science 311:522–527

Cunha AH, Erzini K, Serrão EA, Gonçalves E and others (2014) Biomares, a LIFE project to restore and manage the biodiversity of Prof Luiz Saldanha Marine Park. J Coast Conserv 18:643–655

Di Franco A, Gillanders BM, De Benedetto G, Pennetta A, De Leo GA, Guidetti P (2012) Dispersal patterns of coastal fish: implications for designing networks of marine protected areas. PLoS One 7:e31681

DiBacco C, Levin LA (2000) Development and application of elemental fingerprinting to track the dispersal of marine invertebrate larvae. Limnol Oceanogr 45:871–880

Domingues CP, Nolasco R, Dubert J, Queiroga H (2012) Model-derived dispersal pathways from multiple source populations explain variability of invertebrate larval supply. PLoS One 7:e35794

Fodrie FJ, Becker BJ, Levin LA, Gruenthal K, McMillan PA (2011) Connectivity clues from short-term variability in settlement and geochemical tags of mytilid mussels. J Sea Res 65:141–150

Frieder CA, Gonzalez JP, Levin LA (2014) Uranium in larval shells as a barometer of molluscan ocean acidification exposure. Environ Sci Technol 48:6401–6408

Gaines SD, White C, Carr MH, Palumbi SR (2010) Designing marine reserve networks for both conservation and fisheries management. Proc Natl Acad Sci USA 107: 18286–18293

Gardner J (1992) *Mytilus galloprovincia*lis (Lmk) (Bivalvia, Mollusca): the taxonomic status of the Mediterranean mussel. Ophelia 35:219–243

Gilg MR, Hilbish TJ (2003) The geography of marine larval dispersal: coupling genetics with fine-scale physical ocenography. Ecology 84:2989–2998

Gillanders BM (2002) Temporal and spatial variability in elemental composition of otoliths: implications for determining stock identity and connectivity of populations. Can J Fish Aquat Sci 59:669–679

Keul N, Langer G, de Nooijer LJ, Nehrke G, Reichart GJ, Bijma J (2013) Incorporation of uranium in benthic foraminiferal calcite reflects seawater carbonate ion concentration. Geochem Geophys Geosyst 14: 102–111

Kinlan BP, Gaines SD (2003) Propagule dispersal in marine and terrestrial environments: a community perspective. Ecology 84:2007–2020

Lavín A, Díaz del Río G, Cabanas JM, Casas G (1991) Afloramiento en el noroeste de la península Ibérica Índices de afloramiento para el punto 43°N 11°O periodo 1966–1989. Inf Tec Inst Esp Oceanog no. 91. Instituto Español de Oceanografia, Madrid

Levin LA (2006) Recent progress in understanding larval dispersal: new directions and digressions. Integr Comp Biol 46:282–297

Levin LA, Hoenisch B, Frieder CA (2015) Geochemical proxies for estimating faunal exposure to ocean acidification. Oceanography 28:62–73

Lloyd DC, Zacherl DC, Walker S, Paradis G, Sheehy M, Warner RR (2008) Egg source, temperature and culture seawater affect elemental signatures in *Kelletia kelletii* larval statoliths. Mar Ecol Prog Ser 353:115–130

López-Duarte PC, Carson HS, Cook GS, Fodrie FJ, Becker BJ, DiBacco C, Levin LA (2012) What controls connectivity? An empirical, multi-species approach. Integr Comp Biol 52:511–524

McQuaid CD, Phillips TE (2000) Limited wind-driven dispersal of intertidal mussel larvae: *in situ* evidence from the plankton and the spread of the invasive species *Mytilus galloprovincialis* in South Africa. Mar Ecol Prog Ser 201:211–220

Melton C, Washburn L, Gotschalk C (2009) Wind relaxations and poleward flow events in a coastal upwelling system on the central California coast. J Geophys Res Oceans 114:C11, doi:10.1029/2009JC005397

Miller SH, Morgan SG, White JW, Green PG (2013) Interannual variability in an atlas of trace element signatures for determining population connectivity. Mar Ecol Prog Ser 474:179–190

Mitsuguchi T, Matsumoto E, Abe O, Uchida T, Isdale PJ (1996) Mg/Ca thermometry in coral skeletons. Science 274:961–963

Morgan SG, Fisher JL, Miller SH, McAfee ST, Largier JL (2009) Nearshore larval retention in a region of strong upwelling and recruitment limitation. Ecology 90: 3489–3502

Narváez DA, Navarrete SA, Largier J, Vargas CA (2006) Onshore advection of warm water, larval invertebrate settlement, and relaxation of upwelling off central Chile. Mar Ecol Prog Ser 309:159–173

Nicastro KR, Zardi GI, McQuaid CD, Teske PR, Barker NP (2008) Coastal topography drives genetic structure in marine mussels. Mar Ecol Prog Ser 368:189–195

Nolasco R, Dubert J, Domingues C, Cordeiro Pires A, Queiroga H (2013a) Model-derived connectivity patterns along the western Iberian Peninsula: asymmetrical larval flow and source-sink cell. Mar Ecol Prog Ser 485: 123–142

Nolasco R, Pires AC, Cordeiro N, LeCann B, Dubert J (2013b) A high-resolution modeling study of the Western Iberian Margin mean and seasonal upper ocean circulation. Ocean Dyn 63:1041–1062

Oliveira PB, Nolasco R, Dubert J, Moita T, Peliz Á (2009) Surface temperature, chlorophyll and advection patterns during a summer upwelling event off central Portugal. Cont Shelf Res 29:759–774

Palumbi SR (2004) Marine reserves and ocean neighborhoods: the spatial scale of marine populations and their management. Annu Rev Environ Resour 29: 31–68

Peteiro LG, Labarta U, Fernández-Reiriz MJ, Alvarez-Salgado X, Filgueira R, Piedracoba S (2011) Influence of intermittent-upwelling on *Mytilus galloprovincialis* settlement patterns in the Ría de Ares-Betanzos. Mar Ecol Prog Ser 443:111–127

Philippart CJM, Amaral A, Asmus R, Van Bleijswijk J and others (2012) Spatial synchronies in the seasonal occurrence of larvae of oysters (*Crassostrea gigas*) and mussels (*Mytilus edulis / galloprovincialis*) in European coastal waters. Estuar Coast Shelf Sci 108:52–63

Pineda J, Hare J, Sponaugle S (2007) Larval transport and dispersal in the coastal ocean and consequences for population connectivity. Oceanography 20:22–39

Planes S, Jones GP, Thorrold SR (2009) Larval dispersal connects fish populations in a network of marine protected areas. Proc Natl Acad Sci USA 106:5693–5697

Queiroga H, Cruz T, dos Santos A, Dubert J and others (2007) Oceanographic and behavioural processes affecting invertebrate larval dispersal and supply in the western Iberia upwelling ecosystem. Prog Oceanogr 74: 174–191

R Core Team (2016) R: a language and environment for statistical computing. R Foundation for Statistical Computing, Vienna. https://www.R-project.org

Relvas P, Barton ED (2005) A separated jet and coastal counterflow during upwelling relaxation off Cape Sao Vicente (Iberian Peninsula). Cont Shelf Res 25:29–49

Relvas P, Barton ED, Dubert J, Oliveira PB, Peliz Á, da Silva JCB, Santos AMP (2007) Physical oceanography of the western Iberia ecosystem: latest views and challenges. Prog Oceanogr 74:149–173

Richter TO, De Stigter HC, Boer W, Jesus CC, Van Weering TCE (2009) Dispersal of natural and anthropogenic lead through submarine canyons at the Portuguese margin. Deep Sea Res Part I 56:267–282

Rius M, Cabral HN (2004) Human harvesting of *Mytilus galloprovincialis* Lamarck, 1819, on the central coast of Portugal. Sci Mar 68:545–551

Roberts CM (1997) Connectivity and management of Caribbean coral reefs. Science 278:1454–1457

Roughgarden J, Gaines S, Possingham H (1988) Recruitment dynamics in complex life cycles. Science 241: 1460–1466

Ruiz M, Tarifeño E, Llanos-Riviera A, Padget C, Campos B (2008) Temperature effect in the embryonic and larval development of the mussel, *Mytilus galloprovincialis* (Lamarck, 1819). Rev Biol Mar Oceanogr 43:51–62

Santos-Echeandía J, Caetano M, Brito P, Canario J, Vale C (2012) The relevance of defining trace metal baselines in coastal waters at a regional scale: the case of the Portuguese coast (SW Europe). Mar Environ Res 79:86–99

Send U, Nam S (2012) Relaxation from upwelling: the effect on dissolved oxygen on the continental shelf. J Geophys Res Oceans 117:C04024, doi:10.1029/2011JC007517

Shanks AL, Brink L (2005) Upwelling, downwelling, and cross-shelf transport of bivalve larvae: test of a hypothesis. Mar Ecol Prog Ser 302:1–12

Shanks AL, Grantham BA, Carr MH (2003) Propagule dispersal distance and size and spacing of marine reserves. Ecol Appl 13:159–169

Siegel DA, Mitarai S, Costello CJ, Gaines SD, Kendall BE, Warner RR, Winters KB (2008) The stochastic nature of larval connectivity among nearshore marine populations. Proc Natl Acad Sci USA 105:8974–8979

Simmonds SE, Kinlan BP, White C, Paradis GL, Warner RR, Zacherl DC (2014) Geospatial statistics strengthen the ability of natural geochemical tags to estimate range-wide population connectivity in marine species. Mar Ecol Prog Ser 508:33–51

Smith GK, Guichard F, Petrovi F, McKindsey CW (2009) Using spatial statistics to infer scales of demographic connectivity between populations of the blue mussel, *Mytilus* spp. Limnol Oceanogr 54:970–977

Sordo I, Barton ED, Cotos JM, Pazos Y (2001) An inshore poleward current in the NW of the Iberian Peninsula detected from satellite images, and its relation with *G. catenatum* and *D. acuminata* blooms in the Galician Rias. Estuar Coast Shelf Sci 53:787–799

Sorte CJ, Etter RJ, Spackman R, Boyle EE, Hannigan RE (2013) Elemental fingerprinting of mussel shells to predict population sources and redistribution potential in the Gulf of Maine. PLoS One 8:e80868

Strasser CA, Thorrold SR, Starczak VR, Mullineaux LS (2007) Laser ablation ICP-MS analysis of larval shell in softshell clams (*Mya arenaria*) poses challenges for natural tag studies. Limnol Oceanogr Methods 5:241–249

Swearer SE, Caselle JE, Lea DW, Warner RR (1999) Larval retention and recruitment in an island population of a coral-reef fish. Nature 402:799–802

Swearer SE, Forrester GE, Steele MA, Brooks AJ, Lea DW (2003) Spatio-temporal and interspecific variation in otolith trace-elemental fingerprints in a temperate estuarine fish assemblage. Estuar Coast Shelf Sci 56: 1111–1123

Thorrold SR, Zacherl DC, Levin LA (2007) Population connectivity and larval dispersal using geochemical signatures in calcified structures. Oceanography 20: 80–89

Vaz N, Fernandes L, Leitão PC, Dias JM, Neves R (2009) The Tagus estuarine plume induced by wind and river runoff: winter 2007 case study. J Coast Res 56:1090–1094

Warner RR, Swearer SE, Caselle JE, Sheehy M, Paradis G (2005) Natal trace-elemental signatures in the otoliths of an open-coast fish. Limnol Oceanogr 50:1529–1542

Werner FE, Cowen RK, Paris CB (2007) Coupled biological and physical models present capabilities and necessary developments for future studies of population connectivity. Oceanography 20:54–69

White JW, Ruttenberg BI (2007) Discriminant function analysis in marine ecology: some oversights and their solutions. Mar Ecol Prog Ser 329:301–305

White JW, Botsford LW, Hastings A, Largier JL (2010) Population persistence in marine reserve networks: incorporating spatial heterogeneities in larval dispersal. Mar Ecol Prog Ser 398:49–67

Wing SR, Botsford LW, Largier JL, Morgan LE (1995) Spatial structure of relaxation events and crab settlement in the northern California upwelling system. Mar Ecol Prog Ser 128:199–211

Zacherl DC (2005) Spatial and temporal variation in statolith and protoconch trace elements as natural tags to track larval dispersal. Mar Ecol Prog Ser 290:145–163

Editorial responsibility: James McClintock, Birmingham, Alabama, USA

Submitted: December 8, 2015; Accepted: April 27, 2016
Proofs received from author(s): June 6, 2016